Toward Estimating Current Densities in Magnetohydrodynamic Generators

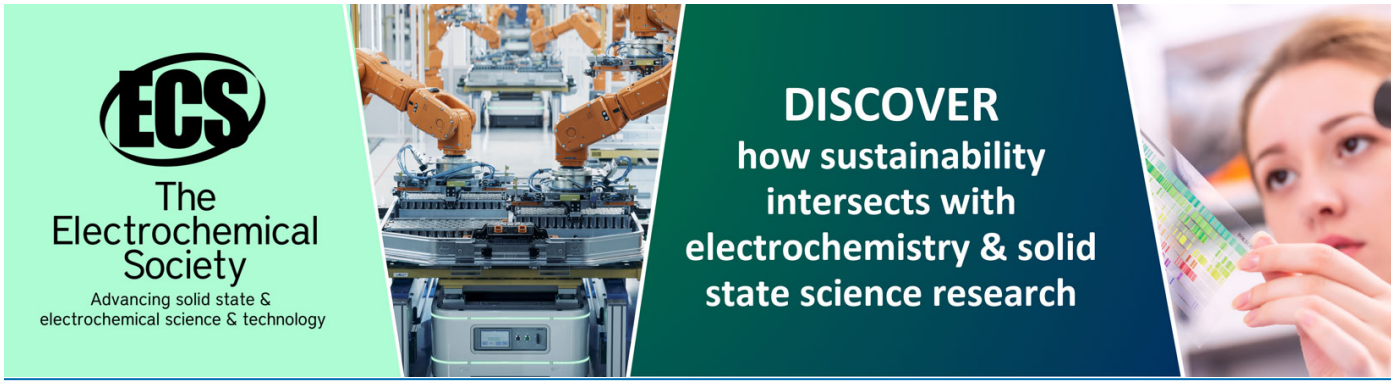

Journal of Physics: Conference Series **640** (2015) 012032 doi:10.1088/1742-6596/640/1/012032

Toward Estimating Current Densities in Magnetohydrodynamic Generators

V. A. Bokil[1], N. L. Gibson[1], D. A. McGregor[1,2] and C. R. Woodside[2]

[1] Oregon State University, Corvallis, OR 97331-4605, USA
[2] National Energy Technology Laboratory, Albany, OR 97321-2198, USA

E-mail: mcgregod@math.oregonstate.edu

Abstract. We investigate the idea of reconstructing current densities in a magnetohydrodynamic (MHD) generator channel from external magnetic flux density measurements in order to determine the existence and location of damaging arcs. We model the induced fields, which are usually neglected in low magnetic Reynold's number flows, using a natural fixed point iteration. Further we present a sensitivity analysis of induced fields to current density profiles in a 3D, yet simplified model.

1. Introduction

Direct power extraction via magnetohydrodynamic (MHD) principles offers a potential step improvement in thermal efficiencies over energy systems utilizing traditional turbomachinery [1]. This is principally due to the lack of moving parts in an MHD generator, as the temperature limits of the moving parts tend to limit cycle temperatures in traditional combustion driven systems. It was established that a major weakness toward commercialization of MHD power generation was the durability of the current collectors on the walls of the generator (electrodes). The electrodes must withstand harsh conditions, and the most damaging and perhaps most difficult to predict phenomenon experienced in the generator was arcing. Consider the example of an oxifuel kerosene MHD Generator with a water-cooled, copper channel. The combustion product will be at approximately 2500 K while the channel will be kept at a temperature near 500 K. This large difference in temperature causes a thermal boundary layer to form in the plasma, where the bulk flow will be much hotter than a thin layer near the edge of this channel. As the plasma is thermally ionized, the conductivity will drop in this boundary layer. Large arcs of high current density will then form near the electrodes as the current which is forced through the electrodes will have to "jump the conductivity gap."

In the arc state we expect the current densities in the channel to be many orders of magnitude larger than in the diffuse state. Given these large differences in current density, the induced magnetic fields are measurably different near the arc. Therefore properties of the current density may be inferred via measurements of the induced fields. The idea of reconstructing current densities from external magnetic flux density measurements has been successfully applied to fuel cells and vacuum arc remelters [2]. The standard approach to this problem is to apply the Biot-Savart law and solve a system of *integral equations*. This formulation unfortunately requires many assumptions on the geometry and the model parameters. Instead, one can formulate the inversion by way of a simulation-based parameter estimation. This technique requires the

simulation of a forward problem whose inputs are parameterized explicitly. One then matches the solution of the model to measured data by minimizing the discrepency between data and simulation using non-linear optimization techniques in the parameter space.

It is our goal here to provide a proof of concept for inversion, via sensitivity analysis, that current densities inside the channel of a magnetohydrodynamic generator (MHDG) can indeed be estimated from external measurements of the induced magnetic fields. This is in comparison to using measurements of the applied field which will most often already be known. It is worth noting that the induced fields are expected to be significantly smaller than the applied field of the generator, which will be a practical issue in the design of experiments.

2. Modeling

A complete description of the bulk flow of a ionized gas in the presence of a magnetic field is governed by a coupling of the Euler Equations to the Maxwell Equations [3]. It is important to observe that many of these parameters, e.g. electrical conductivity, can reasonably be assumed to be constitutive and are truly dependent upon other state parameters, e.g. gas temperature. This implies that the coupling between systems in the equations below may be stronger than is apparent. The following system of partial differential equations can be found in [4]. We use the convention that for a vector field $\mathbf{f}$, the function $\sqrt{\mathbf{f}\cdot\mathbf{f}}$ is referred to as f.

$$\rho\left(\partial_t + \mathbf{u}\cdot\nabla\right)\mathbf{u} = \mathbf{J}\times\mathbf{B} - \nabla p \qquad \text{(Conservation of Momentum)} \quad (2.1a)$$

$$\rho\partial_t\mathcal{E} + \rho\mathbf{u}\cdot\nabla\left(\frac{\mathbf{u}\cdot\mathbf{u}}{2} + U\right) = -\nabla\cdot(\mathbf{u}p) - \nabla\cdot\left(\mu^{-1}\mathbf{E}\times\mathbf{B}\right) \qquad \text{(Conservation of Energy)} \quad (2.1b)$$

$$(\partial_t + \mathbf{u}\cdot\nabla)\rho = -\rho\nabla\cdot\mathbf{u} \qquad \text{(Conservation of Mass)} \quad (2.1c)$$

$$\nabla\times\mu^{-1}\mathbf{B} = \mathbf{J} \qquad \text{(Ampere's Law)} \quad (2.1d)$$

$$\partial_t\mathbf{B} = -\nabla\times\mathbf{E} \qquad \text{(Faraday's Law)} \quad (2.1e)$$

$$\mathbf{J} = \sigma(\mathbf{E} + \mathbf{u}\times\mathbf{B}) + \frac{\beta}{B}\mathbf{J}\times\mathbf{B} \qquad \text{(Ohm's Law with Hall effect)} \quad (2.1f)$$

$$\nabla\cdot\mathbf{B} = 0 \qquad \text{(Gauss' Law for Magnetism)} \quad (2.1g)$$

where, the energy $\mathcal{E}$ is defined as $\mathcal{E} = \dfrac{\mathbf{u}\cdot\mathbf{u}}{2} + U + \dfrac{\epsilon\mathbf{E}\cdot\mathbf{E}}{2} + \dfrac{\mathbf{B}\cdot\mathbf{B}}{2\mu}$. Taking the divergence of Ampere's law gives us the *continuity equation* $\nabla\cdot\mathbf{J} = 0$. The variables in the Hall-MHD system are defined in Table 1.

Table 1. State variables for the Hall-MHD Model (2.1).

$\mathbf{u}$	plasma velocity	U	thermal energy of the plasma
p	pressure	$\mathbf{B}$	magnetic flux density
$\mathbf{E}$	electric field	$\mathbf{J}$	current density
β	Hall parameter	μ	magnetic permeability
σ	electrical conductivity	ρ	plasma density

We make two assumptions which are reasonable for the applications of interest [5].

Assumption 1 : The magnetic field is the sum of applied and induced fields $\mathbf{B} = \mathbf{b}_0 + \mathbf{b}$ where the applied field $\mathbf{b}_0 = (0, 0, b_0)^T$ is constant. In addition we assume that the applied field is of much greater intensity than the induced fields, e.g. $b \ll |b_0|$. The magnetic Reynolds number ($R_m \propto \mu\sigma u$) is known to be much less than one, due to the low conductivity and magnetic permeability, in the case MHD generators and is proportional to the ratio $\frac{b}{|b_0|}$.

Assumption 2 : The generator is in equilibrium, namely that all time derivatives are 0. An argument can be made that if the generator is run for a long time it will reach an equilibrium

state. However, we have little reason to suspect that arcs are not a temporal effect. We make this assumption as a first attempt at understanding the problem and hope to lift this assumption in future work.

By applying these two assumptions to the above model we end up with the following system of equations, in which $\eta = \sigma^{-1}$ and where Poynting's Theorem is used to simplify the right-hand side of (2.1b)

$$\begin{cases} \rho\mathbf{u}\cdot\nabla\mathbf{u} - \nabla p = \mathbf{J}\times\mathbf{b}_0 \\ \rho\mathbf{u}\cdot\nabla\left(\frac{u^2}{2}+T\right) + \nabla\cdot(\mathbf{u}p) = \mathbf{J}\cdot\mathbf{b}_0 \\ \nabla\cdot(\rho\mathbf{u}) = 0 \end{cases} \quad \text{Aerostatic System} \tag{2.2}$$

$$\begin{cases} \nabla\times\mathbf{b} = \mu\mathbf{J} \\ \nabla\cdot\mathbf{b} = 0 \end{cases} \quad \text{Magnetostatic System} \tag{2.3}$$

$$\begin{cases} \nabla\times\eta\mathbf{J} = \nabla\times(\mathbf{u}\times\mathbf{b}_0) + \beta\nabla\times(\eta\mathbf{J}\times\frac{\mathbf{b}_0}{b_0}) \\ \nabla\cdot\mathbf{J} = 0 \end{cases} \quad \text{Current density System} \tag{2.4}$$

We first note that this formulation implies a natural iterative solution technique for the problem, namely that the Aerostatic and magnetostatic systems could each be solved separately assuming the solutions to the others were given. One could then update $\mathbf{J}$ using Ohm's law as a natural fixed point iteration, and then repeat the larger iteration loop. Second, the two assumptions above lead to a situation in which the induced magnetic fields respond to the system state but do not influence it. From this standpoint, the question of whether the induced fields are good candidates for providing observability of the current density, reduces to a question of the sensitivity of the Magnetostatic system to different features of $\mathbf{J}$. We focus on this question for the remainder of this paper.

3. A Numerical Method for the Magnetostatic System

The magnetostatic problem is the classical div-curl system. There are a number of ways to solve for the induced magnetic flux density given $\mathbf{J}$. It follows from the Helmholtz decomposition [6] that since $\mathbf{b}$ is divergence free it must be the curl of some vector potential $\mathbf{a}$. We will assume the *Coulomb gauge*, namely that

$$\mathbf{b} = \nabla\times\mathbf{a} \quad \text{where} \quad \nabla\cdot\mathbf{a} = 0. \tag{3.1}$$

With this choice established we can now rewrite the magnetostatic system as the saddle point problem: Find $(\mathbf{a}, \lambda)$ satisfying

$$\begin{cases} \nabla\times\nabla\times\mathbf{a} + \nabla\lambda = \mu\mathbf{J} \\ \nabla\cdot\mathbf{a} = 0 \end{cases} \tag{3.2}$$

In this formulation we have introduced a *Lagrange multiplier* λ that can be interpreted as a non-physical magnetic pressure. Since, $\nabla\cdot\mathbf{J} = 0$, assuming that $\mathbf{J}$ is smooth, we can show that $\lambda = 0$ in its domain. This ensures that system (3.2) is weakly consistent with the strong formulation of the magnetostatic problem.

We now define function spaces in which we will seek variational solutions to the saddle point problem.

$$\mathbf{H}(\text{curl}, G) = \{\mathbf{c}\in\mathbf{L}^2(G) : \nabla\times\mathbf{c}\in\mathbf{L}^2(G)\} \tag{3.3}$$

$$\mathbf{H}(\text{div}, G) = \{\mathbf{c}\in\mathbf{L}^2(G) : \nabla\cdot\mathbf{c}\in L^2(G)\} \tag{3.4}$$

$$H^1(G) = \{\psi\in L^2(G) : \nabla\psi\in\mathbf{L}^2(G)\} \tag{3.5}$$

$$\mathbf{V} = \{\mathbf{c} \in \mathbf{H}(\text{curl}, G) : \mathbf{c} \times \mathbf{n} = 0 \text{ on } \partial G\} \tag{3.6}$$

$$W = \{\psi \in H^1(G) : \psi = 0 \text{ on } \partial G\} \tag{3.7}$$

We can then pose (3.2) variationally on a smooth domain G as follows

$$\text{Find } (\mathbf{a}, \lambda) \in \mathbf{V} \times W : \begin{cases} \displaystyle\int_G \nabla \times \mathbf{a} \cdot \nabla \times \mathbf{c} + \int_G \nabla\lambda \cdot \mathbf{c} = \int_G \mu \mathbf{J} \cdot \mathbf{c} \\ \displaystyle\int_G \mathbf{a} \cdot \nabla\varphi = 0 \end{cases}, \quad \forall (\mathbf{c}, \varphi) \in \mathbf{V} \times W. \tag{3.8}$$

Under the assumption that $\mathbf{J}$ is in the dual of $\mathbf{V}$, the well-posedness of the variational problem (3.8) can be proved in the framework of the Babuska-Brezzi theory for saddle-point problems [6]. To avoid contamination of the solution due to reflections generated by Dirichlet type boundary conditions for the field $\mathbf{a}$, we will make the computational domain large enough so that our measurements should be far from boundary effects.

3.1. Mimetic Finite Difference Method

To discretize the continuum problem we will use a Mimetic Finite Difference (MFD) method introduced in [6]. The MFD method is, in essence, a generalization of Yee scheme type staggered difference methods to very general geometries. While in our experiments (shown below) we have used Cartesian grids, the nature of these methods is such that they can be easily adapted to the more general geometries which we expect to encounter in practical meshings of a MHD generator channel and casing.

As the details of this method can be found in [6], we will provide here only a brief overview of the method. First consider a given mesh whose nodes we will call $\mathcal{T}_h$, whose edges we will call $\mathcal{E}_h$ and whose faces we will call $\mathcal{F}_h$. On each of these structures there is a natural association with functions H^1, $\mathbf{H}(\nabla\times)$ and $\mathbf{H}(\nabla\cdot)$ respectively. Thus on each structure we assume the following degrees of freedom

$$f \in H^1(G), \quad f_h = (f(\mathbf{x}_i) : \mathbf{x}_i \in \mathcal{T}_h), \tag{3.9}$$

$$\mathbf{v} \in H(\text{curl}, G), \quad \mathbf{v}_h = \left(\frac{1}{|e_i|} \int_{e_i} \tau_i \cdot \mathbf{v} : e_i \in \mathcal{E}_h \text{ and } \tau_i \text{ tangent to } e_i \right), \tag{3.10}$$

$$\mathbf{w} \in H(\text{div}, G), \quad \mathbf{w}_h = \left(\frac{1}{|f_i|} \int_{f_i} \mathbf{n}_i \cdot w : f_i \in \mathcal{F}_h \text{ and } n_i \text{ normal to } f_i \right). \tag{3.11}$$

Given that we will be working with a lowest order method it also natural to then associate edge and face degrees of freedom with midpoints of edges and barycenters of faces as these represent a sufficiently accurate quadrature. We construct, for each set, a mass matrix $\mathbb{Q}_\mathcal{T}, \mathbb{Q}_\mathcal{E}, \mathbb{Q}_\mathcal{F}$ which produces an $\mathcal{O}(h)$ approximation of the L^2 inner product for a form defined on each topology. For example,

$$\mathbf{u}_h, \mathbf{v}_h \in \mathcal{E}_h : \mathbf{v}_h^T \mathbb{Q}_\mathcal{E} \mathbf{u}_h \approx \int_G \mathbf{u} \cdot \mathbf{v} + \mathcal{O}(h). \tag{3.12}$$

These matrices are constructed by producing the matrix on each cell of the discretization and then assembling them in a standard way. One can also construct discrete operators which satisfy analogies of the Fundamental Theorem of Calculus, Stokes Theorem, and Divergence Theorem,

as follows

$$\mathcal{GRAD}_h : \mathcal{T}_h \to \mathcal{E}_h, \mathcal{GRAD}_h f_h = \left(\frac{f(\mathbf{x}_i) - f(\mathbf{x}_j)}{|e_k|} : \text{ for } \mathbf{x}_i, \mathbf{x}_j \text{ the endpoints of } e_k \in \mathcal{E}_h \right) \quad (3.13)$$

$$\mathcal{CURL}_h : \mathcal{E}_h \to \mathcal{F}_h, \mathcal{CURL}_h \mathbf{v}_h = \left(\frac{1}{|f_i|} \sum_{e_j \in f_i} \sigma_{ij} |e_j| \mathbf{v}(e_j) : f_i \in \mathcal{F}_h, \sigma_{ij} = \pm 1 \right). \quad (3.14)$$

Given our assumptions about the continuum problem we will seek $\mathbf{a}_h \in \mathcal{E}_h$ and $\lambda_h \in \mathcal{T}_h$ given $\mathbf{j}_h \in \mathcal{E}_h$. By accounting carefully for where the image of each differential operator lies, one can construct a discrete system as follows

$$\begin{bmatrix} \mathcal{CURL}_h^T \mathbb{Q}_\mathcal{F} \mathcal{CURL}_h & \mathbb{Q}_\mathcal{E} \mathcal{GRAD}_h \\ -\mathcal{GRAD}_h^T \mathbb{Q}_\mathcal{E} & \end{bmatrix} \begin{bmatrix} \mathbf{a}_h \\ \lambda_h \end{bmatrix} = \begin{bmatrix} \mathbb{Q}_\mathcal{E} \mathbf{j}_h \\ 0 \end{bmatrix}. \quad (3.15)$$

With the discrete forward problem posed, we now describe the computation of sensitivities.

4. Sensitivity Analysis

In order to determine the viability of the response of the induced magnetic flux density to changes in the current density we will perform a sensitivity analysis. There are number of features of current densities which are suspected to occur in MHD Generator channels which we would like to be able to detect.

Total Current Given that the current is extracted from the channel by the load applied across the electrodes and will be a design parameter for the generator.

Current Density Experimental evidence from legacy MHD research suggests that the destructive macro-arcs which form at electrodes will much denser current profiles than the diffuse state. As our long term goal is to detect the location of the arcs inside the generator and facilitate an understanding of their dynamics, this is perhaps the most critical parameter for sensitivity.

Direction of Current Density It is known from earlier MHD work that the Hall effect causes a tilt to the current density, pointing the current slightly in the direction of the fluid flow [7]. Sensitivity to this parameter would allow one to estimate the magnitude of the Hall effect near the sensor.

Given these three features, we have developed the following parameterized current profile

$$\mathbf{j}(x, y, z; J_m, s, \theta) = \mathbf{v} \frac{J_m}{\sqrt{2\pi s^2}} \exp\left(\frac{1}{2s^2} \left| (\mathbb{I} - \mathbf{v}\mathbf{v}^T) \begin{bmatrix} x \\ y \\ z \end{bmatrix} \right|^2 \right), \quad \mathbf{v} = \begin{bmatrix} \cos\theta \\ \sin\theta \\ 0 \end{bmatrix}. \quad (4.1)$$

This current density is a Gaussian around the line passing through the origin pointing in the direction $(\cos\theta, \sin\theta, 0)^T$. The parameter J_m (A/m^2) controls the total current in the system, the parameter s (m) controls the spread of the density profile, and θ controls the tilting of the arc due to the Hall effect. A significant feature of this formulation is that the profile is naturally divergence free as all variation happens orthogonally to the direction the vector field is pointing.

To perform our sensitivity analysis we fix two parameters and vary the third. We compute actual magnetic flux density values instead of derivatives in order to additionally inform the necessary specifications of measurement equipment. We assume our domain is $[-0.5, 0.5]^3$, the magnetic permeability is constant and on the order of 10^{-6} (which is on the order of magnitude of air at STP) and we measure the magnetic flux density at $(0, 0.015, 0.015)$ and $(.25, 0.015, 0.015)$.

The center result is to estimate the magnitude of fields very close to the arc, while the short distance away is to demonstrate the effect of measuring outside the channel near where sensors would be placed. The sensitivity results are depicted in Figure 1. Figure 1(a) shows high sensitivity to J_m, while Figure 1(b) shows an increasing sensitivity to s in the limit toward smaller diameter, i.e., dense arcs. Finally, Figure 1(c) shows a significant lack of sensitivity to angle at a short distance from the arc.

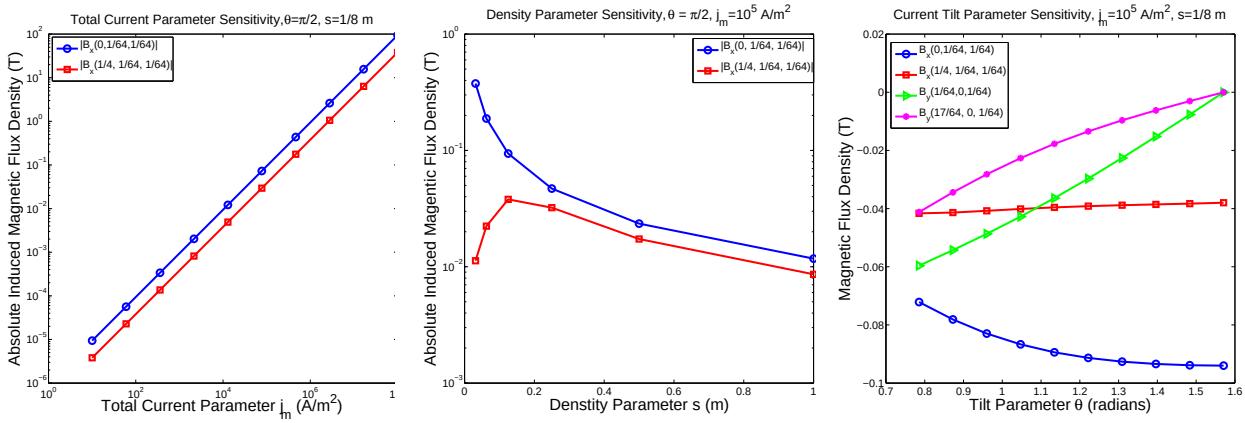

(a) (b) (c)

Figure 1. Analysis of the sensitivity of the induced magnetic flux density to the three current density parameters: J_m, s, and θ.

5. Conclusions

In this paper we have shown that the standard modeling assumptions for the bulk flow of plasma in an MHD generator channel lead to a system in which the induced magnetic flux density responds to the physical system state but does not influence the system. We have created a current density profile which includes several important features of arcs which we wish to be able to detect, namely total current, the direction of the arc, and the width of the density of the arc. Our numerical experiments have confirmed that the magnetic flux density is sensitive to these three features, which is a necessary condition for inversion.

Acknowledgments

This work was supported by the US Department of Energy, National Energy Technology Laboratory grant RES1100426/015.

References

[1] Woodside C R 2012 Direct power extraction with oxy-combustion: An overview of magnetohydrodynamic research activites at the NETL-Regional University Alliance Pittsburgh Coal Conference
[2] Woodside C R and King P 2009 Characterizing arc motion and distribution during vacuum arc remelting *TMS2009 International Symposium on Liquid Metal Processing and Casting. Santa Fe: TMS Publications* vol 75
[3] Davidson P 2001 *An Introduction to Magnetohydrodynamics* (Cambridge University Press)
[4] Rosa R 1987 *Magnetohydrodynamic energy conversion* 2nd ed (McGraw-Hill)
[5] Rosa R J, Krueger C H and Shioda S 1991 *IEEE Trans. Plasma Sci.* **19** 1180–1190
[6] Lipnikov K, Manzini G, Brezzi F and Buff A 2011 *J. Comp. Phys.* **230** 305–328
[7] Huba J D 2003 *Hall Magnetohydrodynamics: A Tutorial* vol LNP 615 (Springer)